

Direct measurement of bulk currents in the quantized Hall regime

S. Sirt,¹ V. Y. Umansky,² A. Siddiki,³ and S. Ludwig^{1,*}

¹Paul-Drude-Institut für Festkörperelektronik, Leibniz-Institut im

Forschungsverbund Berlin e.V., Hausvogteiplatz 5-7, 10117 Berlin, Germany

²Weizmann Institute of Science, 234 Herzl Street, POB 26, Rehovot 76100, Israel

³Istanbul Atlas University, Hamidiye, Anadolu Cd. no:40, 34408, Istanbul, Turkey

The integer quantized Hall effect reveals a state of scattering-free carrier transport and quantized resistance in a two-dimensional conductor exposed to a perpendicular magnetic field. The quantized resistance is observed for the Hall bar geometry, i.e., if the current carrying contacts are connected by sample edges. A widely accepted model is the Landauer-Büttiker picture, which assumes an incompressible, i.e., electrically insulating bulk state surrounded by one-dimensional edge channels giving rise to quantized resistance. This model is challenged by the screening theory, which takes into account electron-electron interaction and predicts for the quantized Hall plateaus current flow in incompressible strips, which gradually shifts from the sample edges into the bulk with increasing magnetic field. We present direct proof of the predicted scattering-free bulk transport by exploring a Hall bar augmented with an additional contact placed in its center away from the Hall bar edges. Our result supports the screening theory.

I. INTRODUCTION

Since its discovery in 1980 by Klaus von Klitzing [1], the integer quantized Hall effect (QHE) has been a subject of fundamental research and provides today the recommended standard for calibrating electrical resistance [2, 3]. The QHE is a manifestation of the Landau quantization of the charge carriers density of states (DOS) when exposed to a magnetic field. Its main features are extended plateaus of the Hall resistance as a function of the magnetic field at quantized values $R_V = R_K/\nu$, where $R_K = h/e^2$ is the fundamental von Klitzing constant and $\nu = 1, 2, 3, \dots$ is the filling factor measuring the fraction of occupied Landau levels. Despite the relative maturity of the QHE, its microscopic nature including the distribution of the scattering-free current at quantized Hall resistance is still controversially discussed. It goes without saying that the microscopic details are important for both, our fundamental understanding of the QHE and our ability to optimize the accuracy of its metrological application. In addition, the question where the current flows is central for possible quantum technology applications, because the phase accumulated by a charge carrier crucially depends on its path way [4, 5].

The Landauer-Büttiker (LB) picture [6, 7] considers non-interacting electrons in equilibrium. It predicts for the entire range of the plateaus chiral current flow through ν compressible quasi one-dimensional (1D) edge channels while the bulk of the sample is incompressible and thereby insulating, caused by the Landau gap of the DOS. The insulating state is thought to be broadened by Anderson localization determining the widths of the plateaus. To then find the correct quantized resistance values, one has to assume that the chiral edge channels are free of scattering. Under this condition, each one carries the quantized conductance of a perfect 1D channel, e^2/h .

The screening theory goes beyond the LB picture as it determines the local electrostatic potential and carrier distribution taking into account the confinement potential, the direct

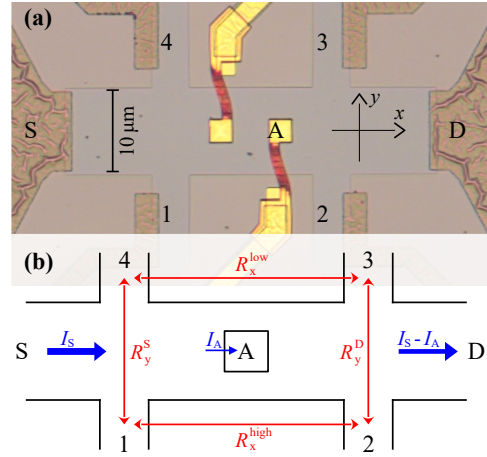


FIG. 1. (a) Microscopic photograph of the sample. The mesa (gray color) shapes the $10\mu\text{m}$ wide Hall bar containing the 2DES at a depth of 130 nm . Where it appears brown and smooth, the surface is etched to a depth of $\approx 240\text{ nm}$. Dark and rough brown regions indicate the ohmic contacts S, D, 1–4. Bright yellow regions indicate the ohmic contacts with air bridges (red) connecting to two inner ohmic contacts (hidden below the squared $2.5\mu\text{m}$ wide gold regions). The left one is always electrically floated (unused), while contact A is connected to ground in some of our measurements. (b) Sketch for orientation: labeling of current contributions and resistance matrix elements as used in the main text; voltage probes 1–4 are floated.

Coulomb interaction of the charge carriers, the applied finite current, optionally disorder, and quantum effects [8–14]. Locally, the Landau quantization gives rise to a bandgap, such that incompressible strips (ICS) emerge coexisting with perfectly screened compressible regions. As a consequence, the electric potential changes in the ICSs only. Accepting that the local electric field is the driving force of the current, the ICS should then carry all the current, while the compressible regions are absolute free of current. Inside the ICSs, the Landau gap prevents scattering and gives rise to the quantized resistance $R_V = R_K/\nu$ [9, 14]. In contrast to LB edge channels, the ICSs are not 1D, indeed the width of an ICS

* sirt@pdi-berlin.de; ludwig@pdi-berlin.de

grows as the magnetic field B is increased along the quantized Hall plateau. While growing wider, the ICSs gradually move from the edge towards the center of the Hall bar, where they combine into a single ICS. The exact position and geometry of the ICSs depend on the local electrostatic potential combining the confinement, the Hall potential, screening via electron-electron interaction, and possibly disorder fluctuations. In contrast to the LB picture, the screening theory predicts plateaus with finite widths even at zero disorder [15].

An increasing number of experiments support the screening theory and thereby provide indirect evidence for current flow inside ICSs [16–23]. Magnetic imaging of a quantum anomalous Hall insulator was interpreted in terms of bulk current [24]. In the present article, we go one step further by performing a direct measurement of bulk current while the Hall resistance is quantized. To achieve this, we use an inner ohmic contact placed near the center of our high-mobility Hall bar. Our result exceeds the scope of the LB picture and supports the screening theory.

II. SETUP

Our $10\mu\text{m}$ wide Hall bar is carved from a GaAs/AlGaAs heterostructure containing a two-dimensional electron system (2DES) 130nm below the surface. We cool it to a temperature of $T \simeq 300\text{mK}$ in a He-3 evaporation cryostat. At this cryogenic temperature, the carrier density and mobility of the 2DES are $n_s \simeq 1.2 \times 10^{11}\text{cm}^{-2}$ and $\mu \simeq 4 \times 10^6\text{cm}^2/\text{Vs}$, respectively, as determined from our Hall measurements. (The corresponding mean-free-path is $\lambda_m \simeq 23\mu\text{m}$.) In Fig. 1(a), we present a micrograph of the Hall bar. It contains two small ohmic contacts close to its center. For this article, the left one is always electrically floated and does not affect the measurements, while in some measurements we connect the contact labeled A to electrical ground.

To perform direct current measurements (using a Keithley 2450 sourcemeter), we apply a constant current $I_S = -100\text{nA}$ (corresponding to $V_S < 0$) through the source contact S, while the drain contact D is always connected to the measurement ground ($V_D = 0$). Note that all ohmic contacts are equipped with standard RC-filters ($R = 2200\Omega$, $C = 2\text{nF}$) for noise reduction and protection from electrostatic discharge damage. Additional cable resistances ($\sim 100\Omega$) and capacitances ($\sim 100\text{pF}$) are much smaller. The resistances of the peripheral ohmic contacts are about 50Ω and that of the inner contact $\simeq 1\text{k}\Omega$, all being almost independent of the magnetic field, B . This adds up to overall contact resistances of $R_i \simeq 2.4\text{k}\Omega$ for the peripheral contacts ($i = 1, 2, 3, 4, \text{S}, \text{D}$) and $R_A \simeq 3.4\text{k}\Omega$ for the inner contact. At $B = 0$, the resistance of the Hall bar itself is $R_0 \simeq 50\Omega$ between contacts S and D.

Contacts 1–4 serve as (electrically floating) voltage probes. We simultaneously measure the four individual voltages $V_{1,2,3,4}$ in respect to ground (employing Agilent 34411A multimeters). Compared to measuring pairwise voltage differences, this increases flexibility but slightly reduces accuracy [25]. In the following, we discuss the four

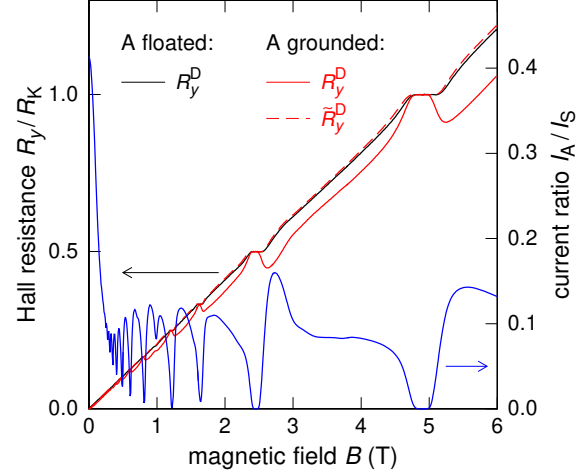


FIG. 2. Left-hand-side axis: measured Hall resistance $R_y^D(B)$ while the inner contact is either floated (black solid line) or grounded (red solid line); the dashed red line is $\tilde{R}_y^D(B)$, corrected for the reduced current. Right-hand-side axis: current ratio I_A/I_S while A is grounded (solid blue line).

terminal resistances $R_{ij} = (V_j - V_i)/I_S$. They include the Hall resistances, which we relabel as $R_{14} = R_y^S$ and $R_{23} = R_y^D$ according to the voltage probe locations near the S versus D contact, and the longitudinal resistances measured along the high-potential versus low-potential edges of the Hall bar, labeled accordingly $R_{12} = R_x^{\text{high}}$ and $R_{43} = R_x^{\text{low}}$, cf. the sketch in Fig. 1(b).

If both, the drain and the inner contact, are connected to electrical ground, we deal with a three-terminal setup. To receive all three currents, we measure in addition to I_S the current flowing through the inner contact I_A using a current amplifier (Basel Precision Instruments).

III. RESULTS

If we keep the inner contact A electrically floating, its influence on the Hall effect measurements can be neglected and we find equal Hall resistances $R_y^S = R_y^D$ and correspondingly identical longitudinal resistances $R_x^{\text{low}} = R_x^{\text{high}}$, as it is expected for a homogeneous carrier density along the Hall bar. For our choice of $V_S < 0$, the source contact has an increased chemical potential and emits electrons. In respect of the flow of these electrons, the Hall resistance R_y^S is measured upstream of contact A and is identical for A being electrically floated or connected to ground. In comparison, R_y^D is measured downstream of A and, therefore, R_y^D , R_x^{high} and R_x^{low} depend on I_A , see Ref. [Supplementary Information] for a complete set of measurements.

In Fig. 2, we show the Hall resistance $R_y^D(B)$ near the drain contact (left axis) for A floated (black line) versus A connected to ground (red solid line). Connecting A to ground yields a reduction of R_y^D whenever $I_A \neq 0$; the blue line in

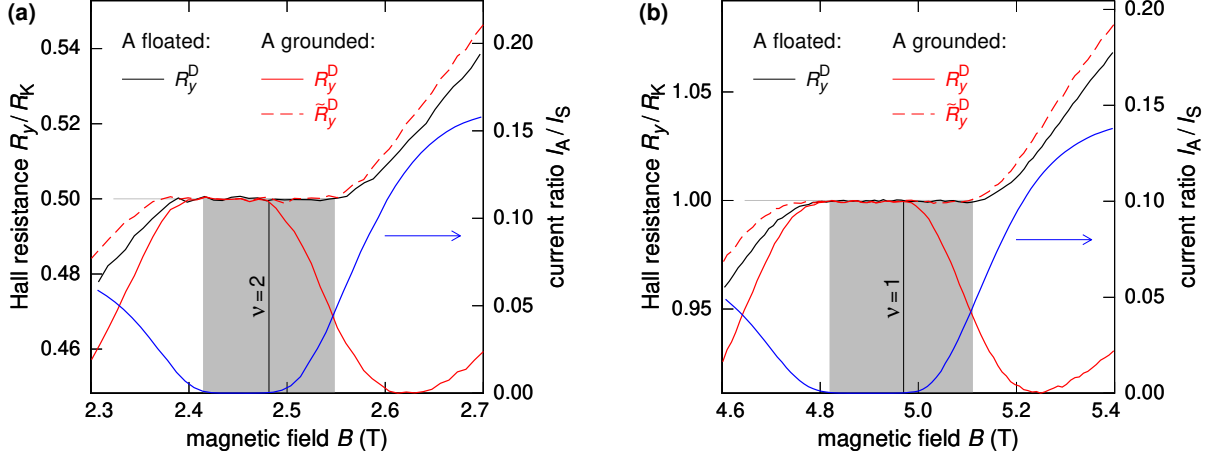


FIG. 3. Enlargements from Fig. 2 (same presentation) near filling factors $\nu = 2$ in (a) and $\nu = 1$ in (b) indicated as vertical lines. The magnetic field regions of the quantized plateaus, as determined for floating A, are depicted as gray background. On the high-field side of the integer bulk filling factor, current flows through contact A while the corrected \tilde{R}_y^D recovers the quantized plateau resistance.

Fig. 2 displays the current ratio $I_A(B)/I_S$ (right axis). We observe a sharp drop of $I_A(B)/I_S$ in the classical regime. For $B > 0.3$ T, these are followed by pronounced Shubnikov-de-Haas oscillations averaging to $I_A \simeq 0.08I_S$. However, I_A vanishes for the largest part of the plateaus, which indicates that the inner contact remains isolated even if grounded. To account for the current reduction downstream of A, we introduce the corrected Hall resistance $\tilde{R}_y^D = R_y^D \frac{I_S}{I_S - I_A}$, which we added in Fig. 2 as a red dashed line. At large, $\tilde{R}_y^D(B)$ recovers $R_y^D(B)$ measured with A floated. However, a detailed look reveals slight deviations and an interesting dynamics.

Focusing on the dynamics in the quantum regime in Fig. 3, we show enlarged sections of the identical data plotted in Fig. 2 covering the first two plateaus near bulk filling factors (averaged over the width of the Hall bar) $\nu = 1$ and $\nu = 2$. The shaded backgrounds indicate the plateau regions for A being floated with $R_y^D = \frac{1}{\nu}h/e^2$ and $R_x^{\text{low}} = R_x^{\text{high}} = 0$. The observed behavior is congruent for $\nu = 1$ and $\nu = 2$.

Throughout the low magnetic field side of the plateaus (for $\nu \gtrsim 1$ or $\nu \gtrsim 2$), the grounded inner contact is electrically isolated with $I_A = 0$ and leaves the quantized Hall plateaus unaffected, i.e., $R_y^D = R_K/\nu$. However, if we increase the magnetic field while remaining on the quantized plateau for $\nu < 1$ or $\nu < 2$, a rapidly growing fraction of the current flows through the inner contact and $R_y^D < R_K/\nu$. Nevertheless, the $I_A \neq 0$ does not affect the quantized Hall state, since the corrected \tilde{R}_y^D exactly recovers the quantized plateau resistance.

IV. DISCUSSION

Our experiments clearly demonstrate that, starting in the middle of the plateau, current flows in the bulk of the Hall bar. Even for $I_A \neq 0$, the QHE does not break down, instead we find $R_y^S = \tilde{R}_y^D = R_K/\nu$. We interpret this finding

in terms of scattering-free bulk current, indeed reaching the inner contact in the center of the Hall bar within the higher-magnetic-field side of the plateau.

While we observe $I_A \neq 0$ only on the higher-magnetic-field halves of the plateaus, the LB picture does not provide a scenario, which breaks the symmetry of the plateaus (in respect to the integer bulk filling factor). Moreover, the only way to interpret an onset of $I_A \neq 0$ based on the LB picture would be the assumption of a breakdown of the QHE induced by the grounded contact A. However, such a breakdown would be accompanied with carrier scattering and would cause a deviation from our finding $R_y^S = \tilde{R}_y^D = R_K/\nu$. We conclude, that the LB picture, which correctly predicts the quantization of the Hall resistance, fails to describe the current density distribution across the Hall bar, which gives rise to the observed asymmetry discussed above.

While the LB picture is a single-particle model, by including electron-electron interactions [8, 14], the screening theory naturally explains a transition along each plateau from scattering-free edge currents to still scattering-free bulk current. This transition causes the asymmetry of $I_A(B)$ and $R_y^D(B)$ in respect to the integer bulk filling factor and also explains a current division free of scattering. In Fig. 4, we qualitatively sketch the prediction of the screening theory for three different filling factors. In Fig. 4(a), we show the situation for $\nu \simeq 1.25$ depicting the diffusive transport regime between plateaus (Drude model), in Fig. 4(b) and 4(c), we sketch typical situations along the quantized plateau, cf. Ref. 26 for comparable numerical calculations. In Fig. 4(b) with $\nu \simeq 1.03$, we consider the low-magnetic-field side of the plateau, where separate narrow ICSs follow along the sample edges. In Fig. 4(c) with $\nu \simeq 0.98$ at the high-field side of the plateau, a single ICS extends through the bulk of the Hall bar. Compressible regions are indicated with light gray shading, ICSs with dark gray shading. Colored striped patterns mark the compressible regions at the highest (red) and lowest (blue) potentials. In Fig. 4(a), the entire Hall bar is

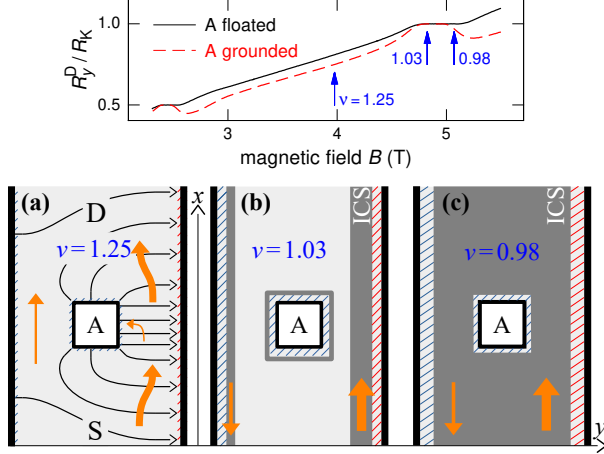


FIG. 4. **Screening theory:** Qualitative sketches of the segmentation of the Hall bar in compressible (light gray) and incompressible (dark gray) regions for contact A connected to ground at three different filling factors near $\nu = 1$ as indicated in the top panel (data from Fig. 2) for orientation. In the sketches, the insulating sample edges and a thin Schottky (tunnel) barrier around A are drawn as black lines. Areas of constant potential (always compressible) near ground are marked by blue stripes, near source (high) potential by red stripes. Orange filled arrows indicate the local flow of electrons. (a) Diffusive regime between plateaus; potential drops gradually across a compressible Hall bar; current flow is uni-directional and perpendicular to the electric field shown as thin black arrows. (b, c) Plateau region; chiral current flow restricted to ICSs; potential changes linearly inside ICSs and is constant in compressible regions; (b) features the case of edge ICSs, which in (c) widened and combined to a single bulk ICS.

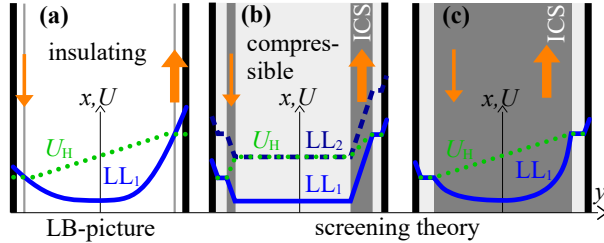


FIG. 5. Sketch of the LL energies across the Hall bar (blue lines solid for LL_1 and dashed for LL_2) and the corresponding Hall potential $U_H(y)$ (dotted green lines). LLs are completely filled at energies below $U_H(y)$, partly filled at $U_H(y)$ and empty above $U_H(y)$. (a) Situation that the LB picture assumes for the entire plateau region (white indicates insulating areas, gray lines perfect 1D edge channels). (b) and (c) Predictions of the screening theory, addressing the low- versus high-magnetic-field sides of the plateau at $\nu \simeq 1$ and corresponding to Figs. 4(b) and 4(c).

compressible, the Hall potential U_H drops across its entire width and current flows everywhere. The according approximate electric field distribution is drawn using thin black arrows, the current flow is indicated by thick orange arrows.

In the case of a quantized plateau as shown in Figs. 4(b) and 4(c), U_H drops entirely inside the ICSs, which are indi-

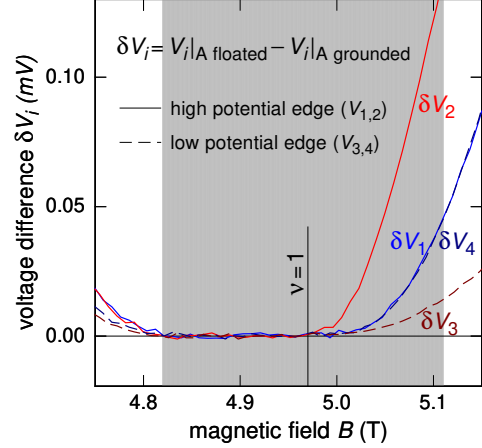


FIG. 6. Voltage differences $\delta V_i = V_i|_{A \text{ floated}} - V_i|_{A \text{ grounded}}$ measured near $\nu = 1$ at the individual contacts for A floated versus grounded. The vertical line indicates the bulk filling factor $\nu = 1$ and the shaded region corresponds to the plateau region for A being floated.

cated using dark gray shading. We plot these Hall potentials $U_H(y)$ together with the course of the $\nu = 1$ LLs in the Figs. 5(b) and 5(c). The current flows where the potential drops, hence, for the plateaus it is restricted to the ICSs. For the case of edge ICSs, cf. Fig. 4(b), the inner contact is isolated and $I_A = 0$. However, in the diffusive regime, cf. Fig. 4(a), or if a bulk ICS exists, cf. Fig. 4(c), current can flow into contact A.

For comparison, in Fig. 5(a), we also present a sketch depicting $U_H(y)$ and the $\nu = 1$ LL as it is expected within the LB picture (uniformly for the entire plateau). In the LB picture, the bulk of the Hall bar is assumed to be insulating, such that current can flow only inside the compressible 1D edge channels. This is in clear contradiction to the prediction of the screening theory, where the current-carrying ICSs with zero resistivity are encompassed by resistive compressible regions free of current.

In the limit of a large magnetic field $\mu B \gg 1$, the current flows perpendicular to the electric field direction, such that most current is guided past contact A. The excess current I_A flowing at large B into A is related with a potential drop along the high-potential edge near A. The potential drop is evident in Fig. 6, in which we plot the individual voltages V_i with $i = 1, 2, 3, 4$. They all decrease with growing I_A/I_S related with the overall decrease of the resistance. This can be seen in Fig. 6 plotting the differences δV_i for A floated versus A grounded exemplary for $\nu = 1$. Within the range of the plateau, we find $\delta V_2 \gg \delta V_1 = \delta V_4 > \delta V_3$. Our finding corresponds to R_x^{high} growing with I_A whilst R_x^{low} lessening (indeed we have $R_x^{\text{high}} - R_x^{\text{low}} = R_y^S - R_y^D$ in accordance with Kirchhoff's voltage law). It implies that a finite I_A yields an increased charge drop and electric field, in particular, along the high-potential edge. In fact, the grounded inner contact largely redistributes the Hall field and, related, the current density across the Hall bar. The potential drop along the

high-potential edge near A is self-consistently related with the current flowing into contact A.

V. SUMMARY AND OUTLOOK

We have performed Hall measurements of a Hall bar equipped with an inner contact, which allows us to directly measure whether current flows in the bulk of the sample. LB edge channels would bypass the inner contact, such that it remained electrically isolated. Our results indicate an asymmetry of the quantized plateaus of the Hall resistance: For the low-magnetic-field side of the plateaus (filling factor exceeding the integer value) the current through the inner contact $I_A = 0$, suggesting that the applied current is restricted to the edges of the Hall bar. In contrast, for the high-magnetic-field side of the plateau (ν lesser than the integer value), we observe $I_A \neq 0$. Here, our results indicate the existence of scattering-free bulk current. Both, bulk current while the resistance is quantized as well as the observed asymmetry of the plateaus with scattering-free bulk current on their high-magnetic-field sides are incompatible with the LB edge channel picture. Our findings confirm the relevance of the electron-electron interactions for the dynamics in the regime of the integer QHE. Our results can be qualitatively explained within the screening theory, which includes the

direct Coulomb interaction between the carriers in a semi-classical approach. A quantitative comparison would require extended numerical calculations, which is beyond the scope of this letter. In future, similar experiments in other material systems confining 2D electrons or holes would be valuable to confirm the generality of our findings.

ACKNOWLEDGEMENT

This work was funded by the Deutsche Forschungsgemeinschaft (DFG, German Research Foundation) – 218453298.

CONTRIBUTIONS OF THE AUTHORS

V. U. produced the sample. S. S. performed the measurements. S. S. and S. L. analyzed the data and wrote the article. A. S. contributed to the planning and provided critical feedback. S. L. led the project.

REFERENCES

-
- [1] K. von Klitzing, G. Dorda, and M. Pepper, New method for high-accuracy determination of the fine-structure constant based on quantized hall resistance, *Phys. Rev. Lett.* **45**, 494 (1980).
 - [2] BIPM, *Le Système international d'unités / The International System of Units ('The SI Brochure')*, ninth ed. (Bureau international des poids et mesures, 2019).
 - [3] F. Delahaye and B. Jeckelmann, Revised technical guidelines for reliable dc measurements of the quantized hall resistance, *Metrologia* **40**, 217 (2003).
 - [4] Y. Ji, Y. Chung, D. Sprinzak, M. Heiblum, D. Mahalu, and H. Shtrikman, An electronic mach–zehnder interferometer, *Nature* **422**, 415–418 (2003).
 - [5] V. J. Goldman and B. Su, Resonant tunneling in the quantum hall regime: Measurement of fractional charge, *Science* **267**, 1010–1012 (1995).
 - [6] M. Büttiker, Four-terminal phase-coherent conductance, *Phys. Rev. Lett.* **57**, 1761 (1986).
 - [7] M. Büttiker, Absence of backscattering in the quantum hall effect in multiprobe conductors, *Phys. Rev. B* **38**, 9375 (1988).
 - [8] D. B. Chklovskii, B. I. Shklovskii, and L. I. Glazman, Electrostatics of edge channels, *Phys. Rev. B* **46**, 4026 (1992).
 - [9] D. B. Chklovskii, K. A. Matveev, and B. I. Shklovskii, Ballistic conductance of interacting electrons in the quantum hall regime, *Phys. Rev. B* **47**, 12605 (1993).
 - [10] M. M. Fogler and B. I. Shklovskii, Resistance of a long wire in the quantum hall regime, *Phys. Rev. B* **50**, 1656 (1994).
 - [11] K. Lier and R. R. Gerhardt, Self-consistent calculations of edge channels in laterally confined two-dimensional electron systems, *Phys. Rev. B* **50**, 7757 (1994).
 - [12] A. Siddiki and R. R. Gerhardt, Thomas-fermi-poisson theory of screening for laterally confined and unconfined two-dimensional electron systems in strong magnetic fields, *Phys. Rev. B* **68**, 125315 (2003).
 - [13] A. Siddiki and R. R. Gerhardt, Incompressible strips in dissipative hall bars as origin of quantized hall plateaus, *Phys. Rev. B* **70**, 195335 (2004).
 - [14] R. R. Gerhardt, The effect of screening on current distribution and conductance quantisation in narrow quantum hall systems, *physica status solidi (b)* **245**, 378 (2008).
 - [15] A. Siddiki and R. R. Gerhardt, Range-dependent disorder effects on the plateau-widths calculated within the screening theory of the iqhe, *International Journal of Modern Physics B* **21**, 1362 (2007).
 - [16] K. L. McCormick, M. T. Woodside, M. Huang, M. Wu, P. L. McEuen, C. Duruo, and J. S. Harris, Scanned potential microscopy of edge and bulk currents in the quantum hall regime, *Phys. Rev. B* **59**, 4654 (1999).
 - [17] P. Weitz, E. Ahlswede, J. Weis, K. Klitzing, and K. Eberl, Hall-potential investigations under quantum hall conditions using scanning force microscopy, *Physica E: Low-dimensional Systems and Nanostructures* **6**, 247 (2000).
 - [18] J. Horas, A. Siddiki, J. Moser, W. Wegscheider, and S. Ludwig, Investigations on unconventional aspects in the quantum hall regime of narrow gate defined channels, *Physica E: Low-dimensional Systems and Nanostructures* **40**, 1130 (2008), 17th International Conference on Electronic Properties of Two-Dimensional Systems.
 - [19] A. Siddiki, J. Horas, J. Moser, W. Wegscheider, and S. Ludwig, Interaction-mediated asymmetries of the quantized hall effect, *EPL (Europhysics Letters)* **88**, 17007 (2009).
 - [20] A. Siddiki, J. Horas, D. Kupidura, W. Wegscheider, and S. Ludwig, Asymmetric nonlinear response of the quantized hall effect, *New Journal of Physics* **12**, 113011 (2010).

- [21] J. Weis and K. von Klitzing, Metrology and microscopic picture of the integer quantum hall effect, *Philosophical Transactions of the Royal Society A: Mathematical, Physical and Engineering Sciences* **369**, 3954 (2011).
- [22] Kendirlik E. M., Sirt S., Kalkan S. B., Dietsche W., Wegscheider W., Ludwig S., and Siddiki A., Anomalous resistance overshoot in the integer quantum Hall effect, *Scientific Reports* **3**, 3133 (2013).
- [23] E. M. Kendirlik, S. Sirt, S. B. Kalkan, N. Ofek, V. Umansky, and A. Siddiki, The local nature of incompressibility of quantum hall effect, *Nature Communications* **8**, 14082 (2017).
- [24] G. M. Ferguson, R. Xiao, A. R. Richardella, D. Low, N. Samarth, and K. C. Nowack, Direct visualization of electronic transport in a quantum anomalous hall insulator, *Nature Materials* **22**, 1100–1105 (2023).
- [25] To explore the highest possible accuracy of our multimeters we calibrated them using the measured Hall resistances of the quantized plateaus. The corrections are $< 1\%$.
- [26] A. Yildiz, D. Eksi, and A. Siddiki, The consequences of bulk compressibility on the magneto-transport properties within the quantized hall state, *Journal of the Physical Society of Japan* **83**, 014704 (2014).

Supplementary information: Direct measurement of bulk currents in the quantized Hall regime

S. Sirt,¹ V. Y. Umansky,² A. Siddiki,³ and S. Ludwig^{1,*}

¹Paul-Drude-Institut für Festkörperelektronik, Leibniz-Institut im

Forschungsverbund Berlin e.V., Hausvogteiplatz 5-7, 10117 Berlin, Germany

²Weizmann Institute of Science, 234 Herzl Street, POB 26, Rehovot 76100, Israel

³Istanbul Atlas University, Hamidiye, Anadolu Cd. no:40, 34408, Istanbul, Turkey

In this supplementary information, we provide a complete set of measurements and discuss additional aspects of the experimental findings complementing the discussion in the main article.

the inner contact is grounded, the current density is reduced on the low-potential side of the Hall bar and accordingly increased on its high-potential side. It confirms our sketch in Fig. 4(a) of the main article.

I. COMPLETE SET OF HALL MEASUREMENTS

In Fig. S1 we sketched the sample including a circuit di-

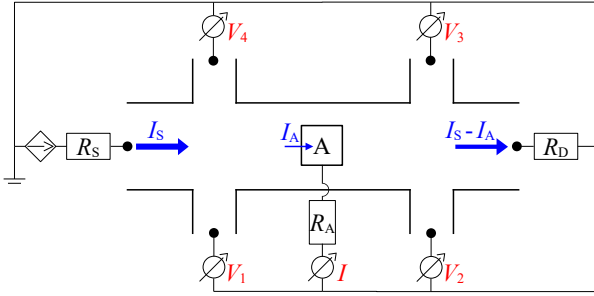


FIG. S1. Sketch of the sample with a simplified circuit diagram of the set-up. The current I_S is applied (and measured) using a constant current source. I_A flowing via the contact resistance R_A to ground is measured as well, if contact A is grounded. The remainder of the current flows via the contact resistance R_D to ground. The voltage probes 1–4 are kept electrically floating, while the voltages $V_{1,2,3,4}$ are simultaneously measured with four separate multimeters.

agram of our measurement set-up. In Fig. S2, we plot both Hall and longitudinal resistances as a function of B while the inner contact A is electrically floated [panel (a)] in comparison to the case when A is connected to ground [panel (b)]. While A is floated, we find the expected relations $R_y^S = R_y^D$ and $R_x^{\text{high}} = R_x^{\text{low}}$, suggesting that our inner contacts do not alter the Hall effect while floated [1]. If we ground the inner contact, R_y^S remains unchanged but we observe $R_y^D \leq R_y^S$ and $R_x^{\text{low}} \leq R_x^{\text{high}}$. The potential differences of a closed loop sum up to zero and, accordingly, we expect $R_y^S - R_y^D = R_x^{\text{high}} - R_x^{\text{low}}$. This is experimentally confirmed in Fig. S3, suggesting that the four individual voltmeters are correctly calibrated. Note that we compared the quantized Hall resistances at the plateaus with the von-Klitzing constant in order to control and, if necessary, fine-tune the calibration of the voltmeters. In the diffusive limit the longitudinal voltage drop difference $R_x^{\text{low}} < R_x^{\text{high}}$ indicates that, while

II. CURRENT THROUGH THE INNER CONTACT

In Fig. S4, we present the measured inner current I_A (μB) for $B \leq 1$ T, an extraction of Fig. 2 of the main article. We observe four different regimes in regard to the current I_A through the inner contact.

- i. *Scattering-free edge current*: within the lower-magnetic-field regions of the plateaus, the entire current flows without scattering along the edges of the Hall bar such that the inner contact is completely isolated and $I_A = 0$, cf. Fig. 3 of the main article.
- ii. *Scattering-free bulk current*: within the higher-magnetic-field regions of the plateaus, the current still flows without scattering but spreads through the bulk of the Hall bar. A fraction of the current flows through the inner contact, cf. Fig. 3 of the main article.
- iii. *Classical regime for $B < 0.3$ T*: at $B = 0$, about 42 % of I_S flows through the inner contact related with the ratio of the contact resistances $R_D \simeq 2.4$ k Ω and $R_A \simeq 3.4$ k Ω . As the magnetic field is increased, I_A/I_S drops to about 8 % in average.
- iv. *Diffusive regime for $B > 0.3$ T*: the Landau quantization causes an oscillation of I_A/I_S around the average value of about 8 %. This oscillation includes the regions of quantized Hall plateaus, regimes i. and ii. above. It also includes regions of diffusive current between the Hall plateaus shaping the local maxima of I_A .

For comparison, the dashed line in Fig. S4 follows a classical approximation for a two-terminal Corbino geometry, $I_A(B)/I_S = \sqrt{(I_A(0)/I_S)^2 + (\mu B)^2/[1 + (\mu B)^2]}$, assuming that for $\mu B \gg 1$ the Hall voltage between the Hall-bar edge and the inner contact drives I_A . The measured initial drop of $I_A(B)$ is much shallower and, even for large B where the current through a Corbino disk vanishes, the average value of the measured I_A remains finite. Clearly, the two-terminal Corbino model does not describe our three-terminal experiment. Deviations are caused by the main fraction of the current, $I_S - I_A$, passing contact A and flowing into the drain contact. Thereby, the grounded contact A modifies the local distribution of the Hall potential. In a hand-waving picture,

* sirt@pdi-berlin.de; ludwig@pdi-berlin.de

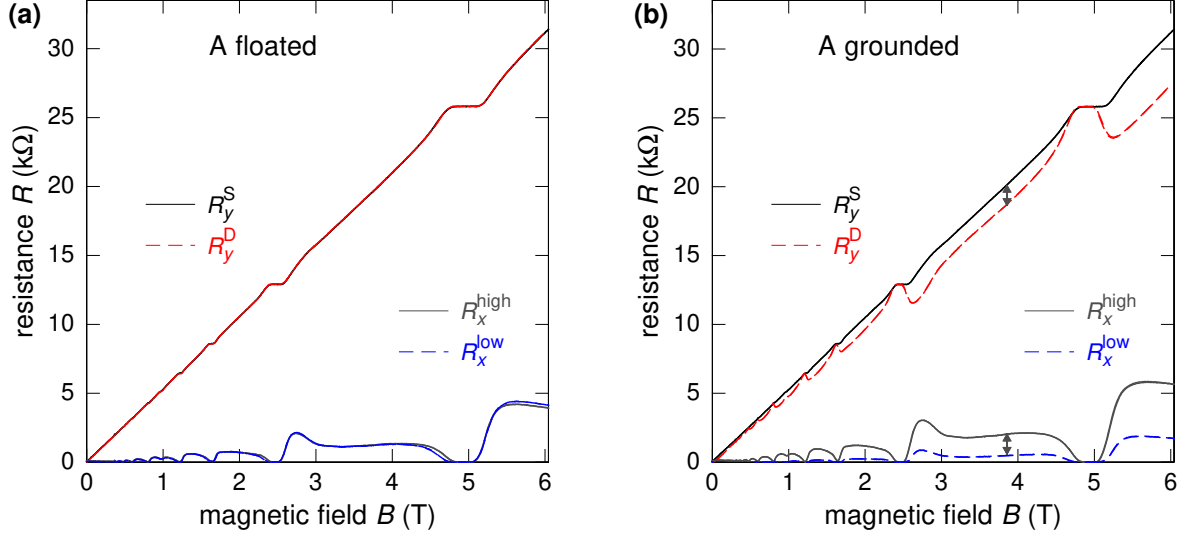


FIG. S2. Hall resistances R_y and longitudinal resistances R_x while the inner contact A is kept electrically floated (a) or connected to ground (b). The two gray double arrows in (b) have identical length.

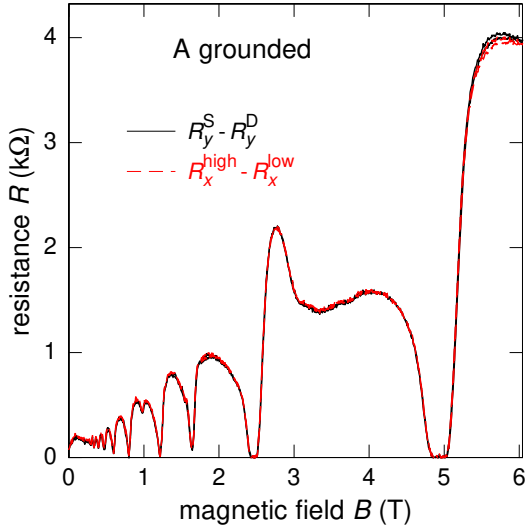


FIG. S3. The inner contact A is connected to ground. The difference between the Hall resistances matches the difference between the longitudinal resistances. After multiplying the resistances with I_S this confirms Kirchhoff's voltage law stating that the direct sum of potential differences around a closed loop is zero.

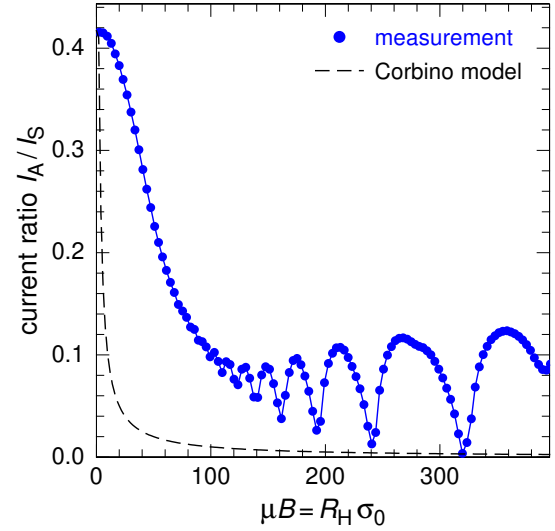


FIG. S4. Ratio of the currents flowing through the inner contact and the source contact I_A/I_S as a function of μB for $B \leq 1$ T. The mobility $\mu = 396 \text{ m}^2/\text{Vs}$ was determined from the Hall measurements. The dashed line follows a model curve assuming a Corbino geometry, cf. main text.

the inner contact blocks the path of the drain current and, hence, even for $\mu B \gg 1$, a sizable fraction of the current flows into the inner contact. This happens, even though the Lorentz force guides most carriers perpendicular to the local electric field, such that they flow around A, cf. Fig. 4(a) of the main article.

In more detail, the current I_A can be seen as part of a self-consistent steady-state solution. It is directly related with

the enhanced voltage drop $V_1 - V_2 \simeq R_H I_A$ along the high-potential edge of the Hall bar. For $\mu B \gg 1$, the corresponding longitudinal electric field drives current perpendicular to the Hall bar edge and into contact A. Therefore, the current I_A depends on the geometry: it would increase for a longer (in x -direction) inner contact. The scenario can be applied to both, the diffusive regime and the case of a bulk ICS, sketched in Fig. 4(a) and Fig. 4(c) of the main article. A

quantitative prediction of the potential distribution and the related current density would require self-consistent numerical calculations.

III. DIFFUSIVE LIMIT OF THE CORRECTED HALL RESISTANCE

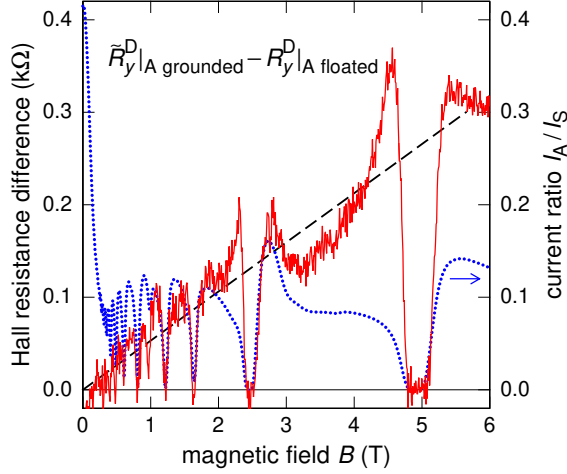


FIG. S5. Difference between the Hall resistances with contact A grounded versus A floated $\tilde{R}_y^D|_{A \text{ grounded}} - R_y^D|_{A \text{ floated}}$ as a function of B (solid red line) and the current $I_A(B)$ flowing through A (dotted line, right-hand-side axis). The black dashed line in the background is proportional to B .

The corrected Hall resistance $\tilde{R}_y^D = R_y^D \frac{I_S}{I_S - I_A} = \frac{V_2 - V_3}{I_S - I_A}$ accounts for the reduced current flowing downstream of the inner contact A. In the diffusive regime (away from the quantized plateaus) we find that \tilde{R}_y^D with $I_A \neq 0$ slightly exceeds $R_H = \frac{B}{en}$. In Fig. S5 we plot $\tilde{R}_y^D|_{A \text{ grounded}} - R_y^D|_{A \text{ floated}}$ in order to visualize this excess Hall resistance. At its local maxima, I_A approximately increases proportional to B and accounts for $\sim 1\%$ of R_y^D . We conjecture that the excess Hall resistance for grounded A is another feature of the self-consistent steady-state solution which also explains I_A . In a nut shell, the voltage drop $V_1 - V_2$ corresponds to a charge density drop along the high-potential edge of the Hall bar. Charge diffusion along the edge then causes an increase of $|V_2|$, which is proportional to R_H , and an according increase of $\tilde{R}_y^D = \frac{V_2 - V_3}{I_S - I_A}$ (note that $|V_3| \simeq 0$).

Another contribution to the observed excess Hall voltage might be a reduced effective carrier density n_s beyond the grounded inner contact. This would be related to the inhomogeneous current distribution across the Hall-bar caused by the grounded inner contact. In particular, an enhanced current near the high-potential edge of the Hall bar, where $n_s(y)$ decreases, yields a decreased average n_s . A quantitative prediction of both discussed effects would require elaborate numerical calculations which go beyond the scope of this article.

[1] To explore the highest possible accuracy of our multimeters we calibrated them using the measured Hall resistances of the quantized plateaus. The corrections are $< 1\%$.